Effective adsorption of nickel (II) with *Ulva lactuca* dried biomass: isotherms, kinetics and mechanisms

Jianyou Long, Xiaona Huang, Xiaoli Fan, Yan Peng and Jianrong Xia

ABSTRACT

This study aimed to evaluate the Ni^{2+} ions adsorption capability of *Ulva lactuca*. The isotherms, kinetics and mechanisms for the adsorption of Ni^{2+} from aqueous solution by *Ulva lactuca* were also investigated. Influencing factors including initial pH, initial Ni^{2+} concentration, biomass, contact time were examined. The results indicate that the maximum Ni^{2+} adsorption capacity of 38.28 mg/g was obtained at pH 5, initial Ni^{2+} concentration 250 mg/L, biomass dosage 0.5 g/L and contact time 30 min. The adsorption can be well fitted with Langmuir isotherm, and the kinetics were well described by the pseudo-second-order model. The parameters of thermodynamics verified that Ni^{2+} adsorption on *Ulva lactuca* was a spontaneous and endothermic process. Analyses of FT-IR, SEM-EDS and XPS indicate that carboxyl and hydroxyl groups on the surface of biomass are involved in Ni^{2+} adsorption. The dried biomass of *Ulva lactuca* can be a cost-effective and eco-friendly adsorbent for the removal of Ni^{2+} from wastewater.

Key words | isotherm, kinetics, mechanisms, Ni^{2+} adsorption, *Ulva lactuca*

Jianyou Long
Xiaona Huang
Xiaoli Fan
Yan Peng
Jianrong Xia (corresponding author)
School of Environmental Science and Engineering,
Guangzhou University,
Guangzhou, 510006,
China
E-mail: *jrxia@gzhu.edu.cn*

Jianyou Long
Key Laboratory for Water Quality and Conservation of the Pearl River Delta, Ministry of Education,
Guangzhou University,
Guangzhou, 510006,
China

Yan Peng
Guangdong Provincial Key Laboratory of radionuclides pollution control and resources,
Guangzhou University,
Guangzhou, 510006,
China

INTRODUCTION

Heavy metal pollution has been a growing concern as a result of rapid industrialization worldwide (Tatsuki *et al.* 2017). Many heavy metals cause a great threat to human and other living organisms because of their carcinogenicity (Ghasemi *et al.* 2011), teratogenicity (Anastopoulos & Kyzas 2015), mutagenicity and biomagnification (He & Chen 2014; Kumar *et al.* 2015) in the food chain. Nickel (II) ions are frequently discharged into the environment from industries such as mineral processing, battery manufacturing, steam-electric power plants and electroplating (Aksu *et al.* 2002; Liu *et al.* 2009; Geetha *et al.* 2016). It can result in different types of disease, e.g. pulmonary fibrosis, renale-dema, skin dermatitis, and gastrointestinal distress (Bulgariu & Bulgariu 2012). Therefore, it is necessary to remove Ni^{2+} from wastewater before discharge.

Conventional techniques for removing heavy metals from water include chemical precipitation (Tang *et al.* 2017), ion exchange (Jayakumar *et al.* 2015), solvent extraction, filtration (Sarı *et al.* 2011), membrane technologies (Oliveira *et al.* 2011) and electrochemical treatment (Tuzen & Sari 2010). But these proposed approaches are usually expensive and not eco-friendly, especially in the treatment of low concentration heavy metal effluents. In recent years, adsorption techniques with some natural biomaterials, including agricultural waste products and seaweeds, were reported to be utilized as adsorbents for the removal of heavy metals from the wastewaters (Vijayaraghavan *et al.* 2006). Among these materials, macroalgal biomass has been proven to be a promising adsorbent in removing heavy metals because of its high adsorption capacity and low cost (Akbari *et al.* 2015). The high adsorption capacity could be mainly attributed to its biochemical constitutions, especially its cell wall, which contains functional groups (such as amino, carboxyl and hydroxyl) that play an important role in the adsorption process (Daneshvar *et al.* 2017; Vijayaraghavan *et al.* 2017). Marine macroalgae can be divided into several sub-groups such as brown algae (Phaeophyta), red algae (Rhodophyta) and green algae (Chlorophyta). Different types of algae have been tested for removal of heavy metals with different effectiveness (Mohammad *et al.* 2014; Gutiérrez *et al.* 2015; Ahmad *et al.* 2016). It has been shown that the inactive biomass may be

doi: 10.2166/wst.2018.253

even more advantageous than active one in the removal of heavy metals because of no biotoxicity concerns and no requirements of growth media (Abdel-Aty *et al.* 2013). Therefore, non-living alga has become one of the popular choices among various adsorbents for disposing the heavy metals from effluents (Nath & Ray 2015).

Ulva lactuca, a green tide alga, widely grew in the southern coast of China with a large biomass. However, only a small portion of *Ulva lactuca* is used for food or forage. The biomass of *Ulva lactuca* was used for Cu^{2+}, Mn^{2+} and Cr^{3+} adsorption (Zeroual *et al.* 2003; Amany *et al.* 2007; Andrew *et al.* 2007). But little attention has been paid to use the algal material as adsorbent for Ni^{2+} removal (Hanan 2008). In the present study, we aimed to test the feasibility of *U. lactuca* as an adsorbent for removing Ni^{2+}. The influencing factors, including initial pH, initial Ni^{2+} concentration, sorbent biomass and contact time, on the adsorption performance were examined. In addition, to gain a better understanding of the adsorption mechanisms, the isotherms, kinetics and thermodynamics were also investigated. The surface structure and functional groups were characterized by scanning electron microscopy (SEM), Fourier transform infrared spectroscopy (FT-IR) and X-ray photoelectron spectroscopy (XPS) analyses.

MATERIALS AND METHODS

Chemicals and reagents

All chemicals and reagents used were of analytical grade and purchased from Guangzhou Huaxin Reagent Co. Ltd, Guangdong, China. Standard solution (1,000 mg/L) of Ni^{2+} was prepared with nickel nitrate ($Ni(NO_3)_2$). The working solution was serially diluted from standard solution daily. The deionized water used in the study was obtained from a deionized (DI) water generator (YL05-20 L 75G, Shenzhen, China).

Preparation of adsorbent

Biomass of *U. lactuca* was collected from Nan Ao Island of Shantou, Guangdong, China. The biomass was cleaned by washing repeatedly with deionized water for removing impurities, and then dried in oven at 80 °C for 6 h. Finally, the dried biomasses were crushed, sieved and stored at room temperature in an airtight container for future use.

Batch adsorption experiments

The batch experiments on Ni^{2+} adsorption were conducted in a temperature-controlled shaker. In order to determine the optimal adsorption conditions, initial pH (2–8), biomass dosage (0.5–5 g/L), initial Ni^{2+} concentration (0–400 mg/L), temperature (288 K, 298 K, 308 K) and contact time (0–250 min) were tested. Solutions of 1 M HCl and 1 M NaOH were used for pH adjustment, and all the experiments were conducted in triplicate.

The concentration of Ni^{2+} was detected by inductively coupled plasma-atomic emission spectroscopy (ICP-AES), and the adsorption capacity of Ni^{2+} was calculated according to the following equation (Lou *et al.* 2015):

$$q_e = \frac{(C_o - C_e)V}{W} \tag{1}$$

where q_e (mg/g) is the adsorption capacity of Ni^{2+}at equilibrium, C_0 and C_e (mg/L) are the initial and equilibrium concentration of Ni^{2+} in the solution, respectively. V (L) is the volume of the aqueous solution, and W (g) is the mass of adsorbent.

Adsorption isotherms

Adsorption isotherm is one important method to illuminate the mechanism of the adsorption systems, which describes how adsorbate interacts with the adsorbent under the equilibrium state (Yeslié *et al.* 2011). In this study, the two most often used adsorption isotherms, namely Langmuir and Freundlich models, were adopted to describe the adsorption process. The Langmuir model defines the monolayer sorption, and could be described by the following equation (Bakatula *et al.* 2014; Li *et al.* 2017a):

$$\frac{C_e}{q_e} = \frac{1}{q_{\max} b} + \frac{C_e}{q_{\max}} \tag{2}$$

where $q_{\max}$ is the maximum biosorption capacity (mg/g) and b is the constant of Langmuir isotherm which is closely related to the energy of adsorption.

The Freundlich model describes the nonideal adsorption on heterogeneous surface as well as multilayer adsorption; its equation is listed below (Zhang *et al.* 2015).

$$\mathrm{In}q_e = \frac{1}{n}\mathrm{In}C_e + \mathrm{In}K_f \tag{3}$$

where K_f (mg/g) is a constant related to the adsorption capacity, n is the constant related to the adsorption intensity.

Adsorption kinetics

In order to evaluate the adsorption rate of Ni^{2+} adsorption, two widely accepted kinetic models, pseudo-first-order and pseudo-second-order were applied to fit the adsorption capacity over the reaction time. The linear equation of pseudo-first-order model is expressed in the following formula (Shroff & Vaidya 2011).

$$\log(q_e - q_t) = \log q_e - \frac{k_1 t}{2.303} \quad (4)$$

where q_t (mg/g) is the adsorption capacity at time t, and k_1 (h^{-1}) is the rate constant. The formula of pseudo-second-order model can be expressed as the following equation (Daneshvar *et al.* 2012).

$$\frac{t}{q_t} = \frac{1}{k_2 q_e^2} + \frac{t}{q_e} \quad (5)$$

where k_2 (g/mg/h) is the second-order rate constant of the adsorption process.

Thermodynamic studies

The thermodynamics for the adsorption of Ni^{2+} onto *Ulva lactuca* were studied at 288 K, 298 K and 308 K, respectively. The thermodynamic parameters change of enthalpy (ΔH^0), entropy (ΔS^0) and Gibbs free energy (ΔG^0) can be calculated from the Equations (6)–(8). (Mitrogiannis *et al.* 2015; Ioannis & George 2016).

$$\Delta G^0 = -\mathrm{RTIn}K_d \quad (6)$$

$$\ln K_d = \frac{\Delta S^0}{R} - \frac{\Delta H^0}{RT} \quad (7)$$

$$\Delta G^0 = \Delta H^0 - T\Delta S^0 \quad (8)$$

where K_d is the equilibrium adsorption distribution constant ($K_d = qe/Ce$), R is the gas constant (8.314 J/mol/K) and T is absolute temperature in Kelvin.

Characterization of *U. lactuca* adsorbent

FT-IR spectra (ALPHA-T, Bruker, Germany) were obtained to explore the surface functional groups presented in *U. lactuca* adsorbent in the range of 400–4,000 cm^{-1}. SEM-EDS (QUANTA200, USA) was used to investigate the morphological characteristics of adsorbent before and after adsorption of Ni^{2+} (Cho *et al.* 2013).

The XPS of adsorbent before and after Ni^{2+} adsorption were obtained by the Theta Probe Angle-Resolved XPS System (hv = 1,486.6 eV, Kratos Axis Ultra, Japan) which was used to identify the element and compounds of *U. lactuca*. Correction of the deviation of the binding energy (BE) owing to the relative surface charging was performed with the C 1 s level at BE of 284.6 eV as an internal standard. The fitting of all XPS spectra was conducted using the software XPSPEAK4.1 (Li *et al.* 2017a, 2017b).

RESULTS AND DISCUSSION

Influence of pH

Many studies have shown that the pH value of solution is one of the key parameters in the adsorption of metal ions which affects the metal binding sites of the sorbent and the metal ion chemistry in aqueous solution (Long *et al.* 2017; Yang *et al.* 2017; Zhang *et al.* 2018). In this study, the influence of initial pH on Ni^{2+} adsorption was conducted by varying the solution pH from 2 to 8 (Figure 1). The adsorption capacity for Ni^{2+} was low at pH less than 3; this could be due to the competition of H^+ over Ni^{2+} to bond the adsorption sites, causing the decrease in Ni^{2+} adsorption performance (Long *et al.* 2017). With the pH increase of the solution, more negatively charged on the surface of *U. lactuca* can be available for the ion-exchange of Ni^{2+}, resulting in the increase of adsorption for Ni^{2+}. As the pH increased the adsorption capacity reached a plateau and no longer increased. This may be explained by the

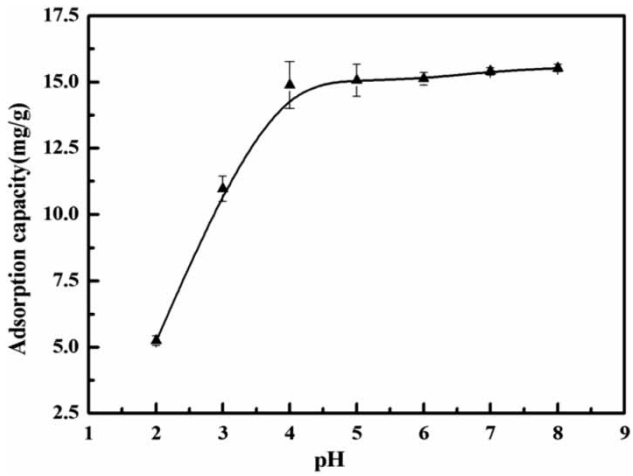

Figure 1 | Influence of solution pH on the adsorption of Ni^{2+} by *U. lactuca*.

formation of soluble hydroxylated complexes of the metal ions and their competition with the active sites on *U. lactuca*, and finally resulting in no increase upon adsorption capacity (Chen *et al.* 2008; Daneshvar *et al.* 2017).

Influence of initial Ni^{2+} concentration

The adsorption capacity increased with the increased Ni^{2+} concentration (Figure 2). This is due to the fact that the increasing initial concentration produces driving force to overcome the mass transfer resistance of Ni^{2+} between the aqueous and solid phase. Then, when the Ni^{2+} concentration further increased from 250 to 400 mg/L, there was no obvious variation on the adsorption efficiency, which may be attributed to the fact that maximum adsorption capacity was reached at the high Ni^{2+} concentration. Similar observations have been found by Tounsadi *et al.* (2015) during biosorption of Cd (II) and Co (II) on *Glebionis coronaria* L. biomasses.

Influence of biosorbent dosage

The biosorbent dosage was also an important parameter affecting the adsorption capacity as well as the removal efficiency. As shown in Figure S1 (available with the online version of this paper), the adsorption capacity decreased gradually as the biomass dosage increased, due to the fact that the adsorption became saturated with increasing adsorbent dosage. The available binding sites for limited adsorbate are excessive when the biomass is in high dosage, and thus leads to the decrease in adsorption capacity during the adsorption process (Christoforidis *et al.* 2015; Chen *et al.* 2008).

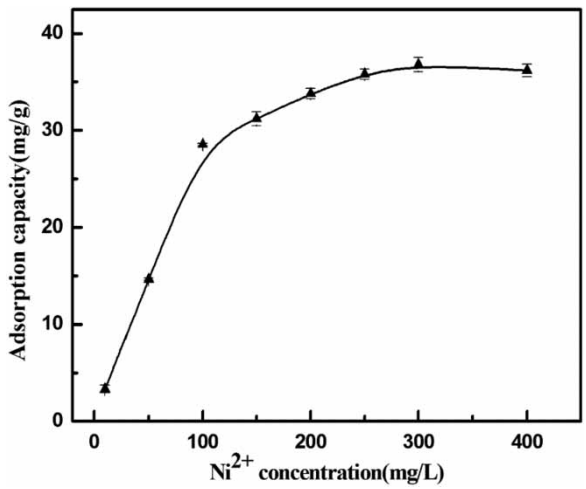

Figure 2 | Influence of initial concentration of Ni^{2+} on the adsorption by *U. Lactuca*.

Influence of contact time

The amount of adsorbed Ni^{2+} increased rapidly during the initial 30 min, and was kept constant when the contact time was further increased (Figure 3). This may be related to the availability of adsorption sites on the biomass surface. At first, adsorption capacity increased quickly owing to sufficient active sites in the beginning; afterward, these active binding sites were gradually occupied (Akbari *et al.* 2015). Therefore, adsorption capacity was kept invariable in the latter adsorption stage.

Adsorption isotherms

For all tested temperatures, the Langmuir model better described the adsorption process with a higher R^2 value of 0.9853, 0.9861 and 0.9819 than the Freundlich model (Table 1 and Figure S2, available online). The maximum adsorption capacity reached 38.28 mg/g at 308 K, and the constant b was 0.0347, respectively. It should be noted that the

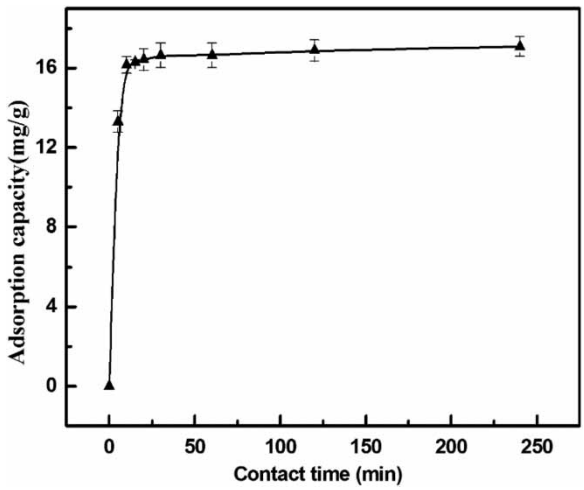

Figure 3 | Influence of contact time on the adsorption of Ni^{2+} by *U. lactuca*.

Table 1 | Isotherm constants for the adsorption of Ni^{2+} by *U. lactuca* at different temperatures

		Temperatures		
Isotherm model	**Parameter**	**288 K**	**298 K**	**308 K**
Langmuir	q_{max}(mg/g)	29.02	32.19	38.28
	b(L/mg)	0.0203	0.0211	0.0347
	R^2	0.9853	0.9861	0.9819
Freundlich	K_f (mg/g)	1.857	1.334	1.363
	n	2.399	1.745	1.722
	R^2	0.9669	0.9534	0.9569

data obtained by both isotherms demonstrate that the higher temperature was more beneficial to the adsorption under the tested conditions, which might indicate the endothermic nature during the adsorption process (Masoumeh *et al.* 2015).

Adsorption kinetics and thermodynamics

The R^2 value (0.999) of the pseudo-second-order kinetic model was higher than that ($R^2 = 0.926$) of pseudo-first-order (Table 2 and Figure S3, available online). This suggests that the pseudo-second-order kinetic model was better in describing the kinetics of Ni^{2+} adsorption. Similar results have been documented for various types of algae adsorbent reported by Pang *et al.* (2011).

The negative value of ΔG^0 at three temperatures (Table 3) indicated that the adsorption of Ni^{2+} was spontaneous (Henriques *et al.* 2015). The positive values of ΔH^0 showed the endothermic nature of the biosorption. The positive values of ΔS^0 suggest increased randomness at the solid/solution interface during the adsorption of Ni^{2+} on the biomass of *U. lactuca*.

Characterization of the adsorbent

FT-IR analysis

The broad and strong peaks around 3,404 cm^{-1} were assigned to the –OH groups (Xu *et al.* 2016) (Figure 4). The bands near 1,652 cm^{-1} could be attributed to the stretching vibration of C=O groups. The band near 1,252 cm^{-1} was assigned to C-O stretching (Castro *et al.* 2017). After Ni^{2+} adsorption, the stretching vibration bands of –OH groups were shifted to 3,384 cm^{-1} for Ni^{2+}-loaded biomass, the peaks of C=O and C-O groups were shifted to 1,639 cm^{-1} and 1,236 cm^{-1}, respectively. This indicates that the chemical interactions between Ni^{2+} and –OH or –NH, C=O and C-O groups of the biomass mainly occurred in the adsorption. The similar FT-IR results were reported for the adsorption of Ni^{2+} on other algae species reported by Castro *et al.* (2017).

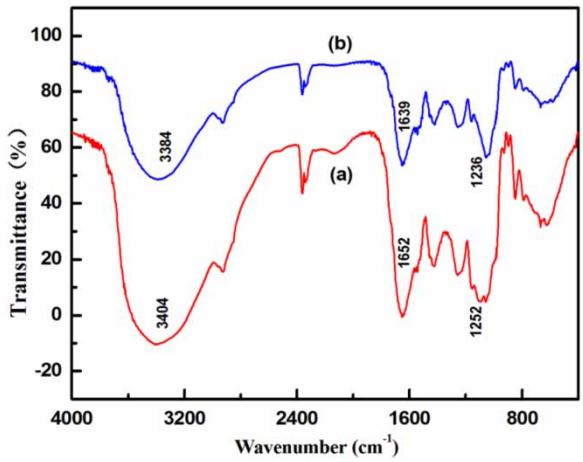

Figure 4 | FT-IR spectra of *U. lactuca* before (a) and after (b) adsorption of Ni^{2+}.

Table 2 | Kinetics constants for the adsorption of Ni^{2+} by *U. lactuca* at different temperatures

		Temperatures		
Kinetics model	**Parameter**	**288 K**	**298 K**	**308 K**
Pseudo-first-order	q_e (mg/g)	10.47	16.34	22.96
	K_1(1/min)	0.1798	0.1833	0.1864
	R^2	0.9142	0.9287	0.9368
Pseudo-second-order	qe (mg/g)	25.23	29.36	35.82
	K_2(g/mg/min)	0.0619	0.0648	0.0723
	R^2	0.9872	0.9913	0.9979

Table 3 | Thermodynamic parameters of Ni^{2+} adsorption by *U. lactuca* at different temperatures

T (K)	$\triangle G^0$(kJ/mol)	$\triangle H^0$(kJ/mol)	$\triangle S^0$(J/mol K)
288	−48.61		
298	−52.28	37.53	0.287
308	−88.86		

SEM-EDS analysis

Before adsorption, the surface of the adsorbent is rough and uneven, surface ridge and void structure decreased after adsorption of Ni^{2+} (Figure 5), as element contents summarized in Table 4. After adsorption, a new peak appears with Ni^{2+} characterization, and the content Ni^{2+} increased by 0.09%, which indicates the successful capture of Ni^{2+} on to the adsorbent (Ramrakhiani *et al.* 2017).

XPS analysis

Figure 6 shows the new characteristic peaks of Ni 3 s and Ni 2P3, which further implies that Ni^{2+} was successfully adsorbed onto the surface of *U. lactuca*. To investigate the mechanism of Ni^{2+} adsorption on *U. lactuca*, the XPS spectra of the C1s, N1s and O1s are analyzed and summarized in Figure S4 (available online). Before adsorption, peaks appeared at 284.8 eV, 285.2 eV and 287.6 eV (Figure S4(a) and S4(b)), which correspond to the functional

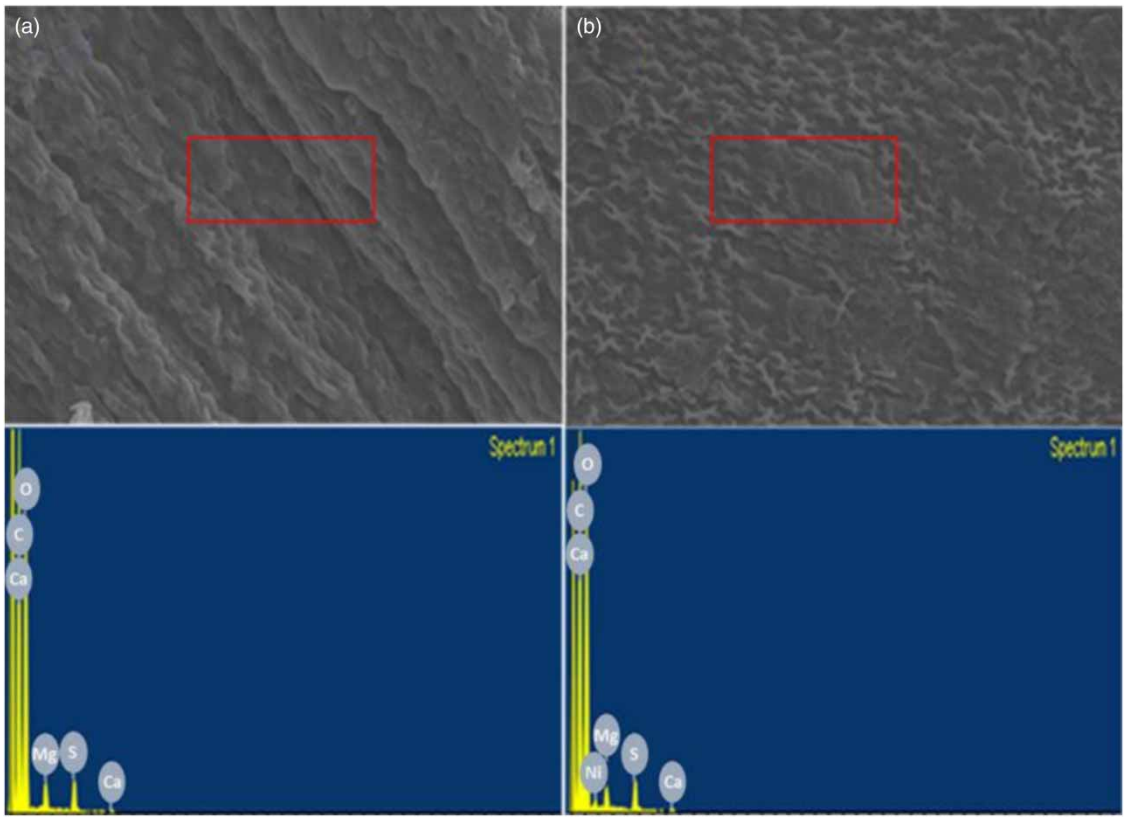

Figure 5 | SEM-EDS photos and spectra of *U. lactuca* before (a) and after (b) adsorption of Ni^{2+}.

groups C-C/C-H, C=O/O-C-O and C-O, respectively (Zhang *et al.* 2017). After adsorption, the peak area of the C-C/C-H and C=O/O-C-O decreased from 37.7% to 35.71%, and from 53.9% to 46.03%, respectively. The peak area of the C-O group increased, indicating that the three functional groups of C-C/C-H, C=O/O-C-O and C-O were involved in the adsorption of Ni^{2+}. The N1S spectra occurred with the characteristic peak of the group $N\text{-}C=O/NH_2$ at 400 eV before adsorption, and a new peak appeared at 400.6 eV after adsorption (Figure S4(c) and S4(d)). In addition, the peak area of the group $N\text{-}C=O/NH_3$ decreased to 91.1%, showing that the functional group of $N\text{-}C=O/NH_3$ is an active site for Ni^{2+} adsorption. Figure S4(e) and S4(f) show that the peak area of group O-H increased from

Table 4 | SEM-EDS quantitative elemental analysis of *U. lactuca* before and after the adsorption of Ni^{2+}

Before element	W%	A%	After element	W%	A%
C K	46.96	54.59	C K	45.79	53.38
O K	50.73	44.27	O K	52.10	45.60
Mg K	1.06	0.61	Mg K	0.86	0.49
S K	1.09	0.48	S K	1.02	0.44
Ca K	0.16	0.06	Ca K	0.15	0.05
Ni K	0	0	Ni K	0.09	0.02
Totals	100.00		Totals	100.00	

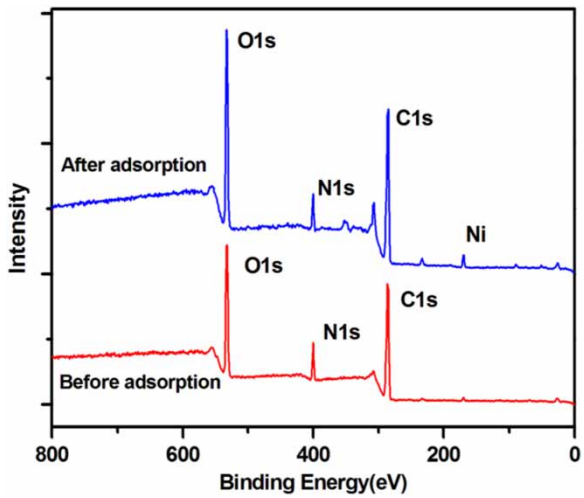

Figure 6 | XPS spectra survey of *U. lactuca* before and after adsorption of Ni^{2+}.

91.28% to 93.7% after adsorption, but the peak area of group C = O/C-O decreased from 8.72% to 6.3%. The group C = O/C-O had a small effect on Ni^{2+} adsorption, which is consistent with the report by Yang *et al.* (2017).

CONCLUSIONS

The dried biomass of *U. lactuca* is found to be an effective, cost-efficient and eco-friendly adsorbent for the removal of Ni^{2+} from aqueous solutions. Maximum adsorption capacity was obtained at pH 5, after 30 min of contact time.

The adsorption of Ni^{2+} can be well described by the Langmuir isotherm model, and the maximum adsorption capacity was 38.28 mg/g. The kinetic studies reveal that the adsorption process fitted the pseudo-second-order kinetic model better than the pseudo-first-order. The calculated values of ΔG and ΔH thermodynamic parameters imply that adsorption process of Ni^{2+} by *U. lactuca* is spontaneous and endothermic. In addition, higher temperature was more favorable to adsorption process. Characterization by FT-IR, SEM-EDS and XPS techniques demonstrates that the functional groups of −OH, N-H, C = O and C-O on the surface of the adsorbent were proven to take part in the adsorption of Ni^{2+}.

ACKNOWLEDGEMENTS

We gratefully acknowledge the financial support provided by National Natural Science Foundation of China (41376156), Guangzhou Science and Technology Program (201510010204, 201804010281), Guangdong innovation platform characteristic innovation project (2016KTSCX106), Guangzhou city science and technology project (201804010281), the Project of Education Bureau of Guangzhou City (1201620219) and the high level university construction project (regional water environment safety and water ecological protection).

REFERENCES

Abdel-Aty, A. M., Ammar, N. S., Ghafar, H. H. A. & Ali, R. K. 2013 Biosorption of cadmium and lead from aqueous solution by fresh water alga *Anabaena sphaerica* biomass. *Journal of Advanced Research* **4** (4), 367–374.

Ahmad, E., Seyedenayat, H., Samad, A. & Bahman, R. 2016 Modification of green algae harvested from the Persian Gulf by L-cysteine for enhancing copper adsorption from wastewater: experimental data. *Cheimical Date Collections* **2**, 36–42.

Akbari, M., Hallajisani, A., Keshtkar, A. R., Shahbeig, H. & Ghorbanian, S. A. 2015 Equilibrium and kinetic study and modeling of Cu(II) and Co(II) synergistic biosorption from Cu(II)-Co(II) single and binary mixtures on brown algae *C. indica*. *Journal of Environmental Chemical Engineering* **3** (1), 140–149.

Aksu, Z., Açıkel, Ü., Kabasakal, E. & Tezer, S. 2002 Equilibrium modelling of individual and simultaneous biosorption of chromium (VI) and nickel (II) onto dried activated sludge. *Water Research* **36** (12), 3063–3073.

Amany, E., Ahmed, E., Azza, K. & Ola, A. 2007 Removal of toxic chromium from wastewater using green alga *Ulva lactuca* and its activated carbon. *Journal of Hazardous Material* **148** (1–2), 216–228.

Anastopoulos, I. & Kyzas, G. Z. 2015 Progress in batch biosorption of heavy metals onto algae. *Journal of Molecular Liquids* **209**, 77–86.

Andrew, T., Marie, S. L., Leyla, S. & Murray, T. B. 2007 Uptake of platinum group elements by the marine macroalga, *Ulva lactuca*. *Marine Chemistry* **105** (3–4), 271–280.

Bakatula, E. N., Cukrowska, E. M., Weiersbye, I. M., Mihaly-Cozmuta, L., Peter, A. & Tutu, H. 2014 Biosorption of trace elements from aqueous systems in gold mining sites by the filamentous green algae (*Oedogonium sp.*). *Journal of Geochemical Exploration* **144**, 492–503.

Bulgariu, D. & Bulgariu, L. 2012 Equilibrium and kinetics studies of heavy metal ions biosorption on green algae waste biomass. *Bioresource Technology* **103** (1), 489–493.

Castro, L., Bonilla, L. A., González, F., Ballester, A., Blázquez, M. L. & Muñoz, J. A. 2017 Continuous metal biosorption applied to industrial effluents: a comparative study using an agricultural by-product and a marine alga. *Environmental Earth Science* **76**, 491–502.

Chen, Z., Ma, W. & Han, M. 2008 Biosorption of nickel and copper onto treated alga (*Undaria pinnatifida*): application of isotherm and kinetic models. *Journal of Hazardous Materials* **155**, 327–333.

Cho, H. J., Baek, K., Jeon, J. K., Park, S. K., Suh, D. J. & Park, Y. 2013 Removal characteristics of copper by marine macro-algae-derived chars. *Chemical Engineering Journal* **217**, 205–211.

Christoforidis, A. K., Orfanidis, S., Papageorgiou, S. K., Lazaridou, A. N., Favvas, E. P. & Ch, Mitropoulos A.,. 2015 Study of Cu(II) removal by *Cystoseira crinitophylla* biomass in batch and continuous flow biosorption. *Chemical Engineering Journal* **277**, 334–340.

Daneshvar, E., Kousha, M., Jokar, M., Koutahzadeh, N. & Guibal, E. 2012 Acidic dye biosorption onto marine brown macroalgae: isotherms, kinetic and thermodynamic studies. *Chemical Engineering Journal* **204**, 225–234.

Daneshvar, E., Vazirzadeh, A., Niazi, A., Sillanpää, M. & Bhatnagar, A. 2017 A comparative study of methylene blue biosorption using different modified brown, red and green macroalgae – effect of pretreatment. *Chemical Engineering Journal* **307**, 435–446.

Geetha, P., Latha, M. S., Pillai, S. S., Deepa, B., Kumar, K. S. & Koshy, M. 2016 Green synthesis and characterization of alginate nanoparticles and its role as a biosorbent for Cr(VI) ions. *Journal of Molecular Structure* **1105** (12), 54–60.

Ghasemi, M., Keshtkar, A. R., Dabbagh, R. & Safdari, S. J. 2011 Biosorption of uranium(VI) from aqueous solutions by Ca-pretreated *Cystoseira indica* alga: breakthrough curves studies and modeling. *Journal of Hazardous Materials* **189** (1–2), 141–149.

Gutiérrez, C., Hansen, H. K., Hernández, P. & Pinilla, C. 2015 Biosorption of cadmium with brown macroalgae. *Chemosphere* **138**, 164–169.

Hanan, H. O. 2008 Biosorption of copper, nickel and manganese using non-living biomass of marine alga, *Ulva lactuca*. *Journal of Biological Sciences* **11**, 964–973.

He, J. & Chen, J. P. 2014 A comprehensive review on biosorption of heavy metals by algal biomass: materials, performances, chemistry, and modeling simulation tools. *Bioresource Technology* **160** (6), 67–78.

Henriques, B., Rocha, L. S., Lopes, C. B., Figueira, P., Rui, J. R. M., Duarte, A. C., Pardal, M. A. & Pereira, E. 2015 Study on bioaccumulation and biosorption of mercury by living marine macroalgae: prospecting for a new remediation biotechnology applied to saline waters. *Chemical Engineering Journal* **281**, 759–770.

Ioannis, A. & George, Z. K. 2016 Are the thermodynamic parameters correctly estimated in liquid-phase adsorption phenomena? *Journal of Molecular Liquids* **218**, 174–185.

Jayakumar, R., Rajasimman, M. & Karthikeyan, C. 2015 Optimization, equilibrium, kinetic, thermodynamic and desorption studies on the sorption of Cu(II) from an aqueous solution using marine green algae: *Halimeda gracilis*. *Ecotoxicology and Environmental Safety* **121** (S12), 199–210.

Kumar, K. S., Dahms, H.-U., Won, E.-J., Lee, J.-S. & Shin, K.-H. 2015 Microalgae – A promising tool for heavy metal remediation. *Ecotoxicology and Environmental Safety* **113**, 329–352.

Li, H. S., Chen, Y. H., Long, J. Y., Jiang, D. Q., Liu, J., Li, S. J., Qi, J. Y., Zhang, P., Wang, J., Gong, J., Wu, Q. H. & Chen, D. 2017a Simultaneous removal of thallium and chloride from a highly saline industrial wastewater using modified anion exchange resins. *Journal of Hazardous Materials* **333**, 179–185.

Li, H. S., Chen, Y., Long, J. Y., Li, X. W., Jiang, D. Q., Zhang, P., Qi, J. Y., Huang, X. X., Liu, J., Xu, R. B. & Gong, J. 2017b Removal of thallium from aqueous solutions using Fe-Mn binary oxides. *Journal of Hazardous Materials* **338**, 296–305.

Liu, Y. H., Cao, Q. L., Luo, F. & Chen, J. 2009 Biosorption of Cd^{2+}, Cu^{2+}, Ni^{2+} and Zn^{2+} ions from aqueous solutions by pretreated biomass of brown algae. *Journal of Hazardous Materials* **163** (2–3), 931–938.

Long, J. Y., Li, H. S., Jiang, D. Q., Luo, D. G., Chen, Y. H., Xia, J. R. & Chen, D. Y. 2017 Biosorption of strontium(II) from aqueous solutions by *Bacillus cereus* isolated from strontium hyperaccumulator *Andropogon gayanus*. *Process Safety and Environmental Protection* **111**, 23–30.

Lou, Z. N., Wang, J., Jin, X. D., Wan, L., Wang, Y., Chen, H., Shan, W. J. & Xiong, Y. 2015 Brown algae based new sorption material for fractional recovery of molybdenum and rhenium from wastewater. *Chemical Engineering Journal* **273**, 231–239.

Masoumeh, A., Ahmad, H., Ali, R. K., Hossein, S. & Sohrab, A. G. 2015 Equilibrium and kinetic study and modeling of Cu(II) and Co(II) synergistic biosorption from Cu(II)-Co(II) single and binary mixtures on brown algae *C. indica*. *Journal of Environmental Chemical Engineering* **3**, 140–149.

Mitrogiannis, D., Markou, G., Çelekli, A. & Bozkurt, H. 2015 Biosorption of methylene blue onto *Arthrospira platensis* biomass: kinetic, equilibrium and thermodynamic studies. *Journal of Environmental Chemical Engineering* **3**, 670–680.

Mohammad, H., Hanafy, H. & Hassan, H. 2014 Remediation of lead by pretreated red algae: adsorption isotherm, kinetic, column modeling and simulation studies. *Green Chemistry Letters and Reviews* **7**, 342–358.

Nath, J. & Ray, L. 2015 Biosorption of Malachite green from aqueous solution by dry cells of *Bacillus cereus* m^{1}_{16} (MTCC 5521). *Journal of Environmental Chemical Engineering* **3** (1), 386–394.

Oliveira, R. C., Jouannin, C., Guibal, E. & Jr, O. G. 2011 Samarium (III) and praseodymium(III) biosorption on *Sargassum sp.*: batch study. *Process Biochemistry* **46** (3), 36–744.

Pang, C., Liu, Y. H., Cao, X. H., Li, M., Huang, G. L., Hua, R., Wang, C. X., Liu, Y. T. & An, X. F. 2011 Biosorption of uranium (VI) from aqueous solution by dead fungal biomass of *Penicillium citrinum*. *Chemical Engineering Journal* **170**, 1–6.

Ramrakhiani, L., Halder, A., Majumder, A., Mandal, A. K., Majumdar, S. & Ghosh, S. 2017 Industrial waste derived biosorbent for toxic metal remediation: mechanism studies and spent biosorbent management. *Chemical Engineering Journal* **308**, 1048–1064.

Sarı, A., Uluozlü, Ö. D. & Tüzen, M. 2011 Equilibrium, thermodynamic and kinetic investigations on biosorption of arsenic from aqueous solution by algae (*Maugeotia genuflexa*) biomass. *Chemical Engineering Journal* **167** (1), 155–161.

Shroff, K. A. & Vaidya, V. K. 2011 Kinetics and equilibrium studies on biosorption of nickel from aqueous solution by dead fungal biomass of *Mucor hiemalis*. *Chemical Engineering Journal* **171**, 1234–1245.

Tang, J., Li, Y., Wang, X. & Daroch, M. 2017 Effective adsorption of aqueous Pb^{2+} by dried biomass of Landoltia punctata and Spirodela polyrhiza. *Journal of Cleaner Production* **145**, 25–34.

Tatsuki, K., Makoto, N., Yoshihiro, K., Atsushi, I., Kota, A., Syuji, M., Katsunori, T., Hitoshi, K. & Jun, T. 2017 Biosorption of metal elements by exopolymer nanofibrils excreted from Leptothrix cells. *Water Research* **122**, 139–147.

Tounsadi, H., Khalidi, A., Abdennouri, M. & Barka, N., 2015 Biosorption potential of *Diplotaxis harra* and *Glebionis coronaria* L. biomasses for the removal of Cd(II) and Co(II) from aqueous solutions. *Journal of Environmental Chemical Engineering* **3**, 822–830.

Tuzen, M. & Sari, A. 2010 Biosorption of selenium from aqueous solution by green algae (*Cladophora hutchinsiae*) biomass: equilibrium, thermodynamic and kinetic studies. *Chemical Engineering Journal* **158** (2), 200–206.

Vijayaraghavan, K., Padmesh, T. V. N., Palanivelu, K. & Velan, M. 2006 Biosorption of nickel(II) ions onto *Sargassum wightii*: application of two-parameter and three parameter isotherm models. *Journal of Hazardous Materials* **133** (1–3), 304–308.

Vijayaraghavan, K., Rangabhashiyam, S., Ashokkumar, T. & Arockiaraj, J. 2017 Assessment of samarium biosorption from aqueous solution by brown macroalga *Turbinaria conoides*. *Journal of the Taiwan Institute of Chemical Engineers* **74**, 113–120.

Xu, L., Chen, X., Li, H. X., Hu, F. & Liang, M. X. 2016 Characterization of the biosorption and biodegradation properties of *Ensifer adhaerens*: a potential agent to remove polychlorinatedbiphenyls from contaminated water. *Journal of Hazardous Materials* **302**, 314–322.

Yang, W. C., Tian, S. Q., Tang, Q. Z., Chai, L. Y. & Wang, H. Y. 2017 Fungus hyphae-supported alumina: an efficient and reclaimable adsorbent for fluoride removal from water. *Journal of Colloid and Interface Science* **496**, 496–504.

Yeslié, G. B., Ivan, L. R., Omar, G. B. & Eric, G. 2011 Nickel biosorption using *Gracilaria caudata* and *Sargassum muticum*. *Chemical Engineering Journal* **166**, 122–131.

Zeroual, Y., Moutaouakkil, A., Dzairi, F. Z., Talbi, M., Chung, P. U., Lee, K. & Blaghen, M. 2003 Biosorption of mercury from aqueous solution by Ulva lactuca biomass. *Bioresource Technology* **90** (3), 349–351.

Zhang, D. N., Ran, Y., Cao, X. Y., Mao, J. D., Cui, J. F. & Schmidt-Rohr, K. 2015 Biosorption of nonylphenol by pure algae, field-collected planktons and their fractions. *Environmental Pollution* **198**, 61–69.

Zhang, B. P., Ma, Z. C., Yang, F., Liu, Y. & Guo, M. C. 2017 Adsorption properties of ion recognition rice straw lignin on $PdCl_4^{2-}$: equilibrium, kinetics and mechanism. *Colloids and Surfaces A: Physicochem. Eng. Aspects* **514**, 260–268.

Zhang, G., Fan, F., Li, X., Qi, J. & Chen, Y. 2018 Superior adsorption of thallium (I) on titanium peroxide: performance and mechanism. *Chemical Engineering Journal* **331**, 471–479.

First received 13 October 2017; accepted in revised form 24 May 2018. Available online 14 June 2018